

CONFIGURATION CONTROL OF ROVER-MOUNTED MANIPULATORS

Homayoun Seraji
Jet Propulsion Laboratory
California Institute of Technology
Pasadena, CA 91109, USA

Abstract

This paper presents a simple on-line approach for motion control of rover-mounted manipulators. An integrated kinematic model of the rover-plus-manipulator system is derived which incorporates the non-holonomic rover constraint with the end-effector task. The redundancy introduced by the rover mobility is exploited to perform a set of user-specified additional tasks during the end-effector motion. The configuration control approach is utilized to satisfy the non-holonomic rover constraint, while accomplishing the end-effector motion and the redundancy resolution goals simultaneously. This framework allows the user to assign weighting factors to the rover movement and manipulator motion, as well as to each task specification. The computational efficiency of the control scheme makes it particularly suitable for real-time implementation. The proposed method is applied to a planar two-jointed arm mounted on a rover, and computer simulation results are presented for illustrational

1 Introduction

In recent years, path planning and motion control of mobile robots have been active areas of research [see, e.g., 1-13]. When the base mobility is provided by a track, a gantry, or another robot, the kinematics of the base platform has holonomic constraints similar to the kinematics of the manipulator itself; thus the base can effectively be treated as additional revolute or prismatic joints of the manipulator [6]. On the other hand, wheeled mobile platforms, such as rovers, are subject to non-integrable kinematic constraints, known as *non-holonomic constraints*. Such constraints are generally

caused by one or several *rolling contacts* between rigid bodies, and reflect the fact that the mobile platform must move in the direction of its main axis of symmetry. A rover is a typical non-holonomic mechanical system. It can attain any position in the plane of motion with any orientation; hence the configuration space is three-dimensional. However, the velocity of motion must always satisfy a non-holonomic constraint; thus the space of achievable velocities is two-dimensional.

In this paper, the configuration control methodology developed earlier [14-15] for redundant robot control is extended to motion control of rover-mounted manipulators. The non-holonomic kinematic constraint of the rover fits naturally in the configuration control formulation. The non-holonomic rover constraint, the desired end-effector motion, and the user-specified redundancy resolution goals are combined to form a set of differential kinematic equations. These equations are then solved to obtain the required rover and manipulator motions.

2 Kinematic Analysis of Rover-Manipulator System

In this section, we develop a fully *integrated* kinematic representation of the rover and the manipulator, rather than treating the rover and the manipulator as two separate entities.

2.1 Non-holonomic Rover Subsystem

Consider a front-wheel-drive four-wheeled rover. The rover is represented by a two-dimensional rectangular object translating and rotating in the plane of motion, as illustrated in Figure 1. Let $F(x_f, y_f)$ denote the midpoint between the two front wheels and $R(x_r, y_r)$ represent the midpoint between the two rear wheels of the rover, where the coordinates are expressed with respect to the fixed world frame $\{W\}$ with axes $(0x, 0y)$

¹The research described in this paper was carried out at the Jet Propulsion Laboratory, California Institute of Technology, under contract with the National Aeronautics and Space Administration.

shown in Figure 1. The rover configuration is parameterized by the 3×1 vector $p = [x_f, y_f, \phi]^T$, where ϕ denotes the orientation of the main axis of the rover relative to the z-axis of the world frame.

Assuming a pure rolling contact between the rover wheels and the ground - i.e., no slipping - the velocity of point R is always along the main axis of the rover. Hence, we have

$$\dot{x}_r = \lambda \cos \phi ; \quad \dot{y}_r = \lambda \sin \phi \quad (1)$$

where λ is a scalar. Eliminating λ , we obtain

$$\dot{x}_r \sin \phi - \dot{y}_r \cos \phi = 0 \quad (2)$$

Equation (2) can be expressed in terms of the coordinates (x_f, y_f) of the front point F on the rover. The coordinates of the rear point $R(x_r, y_r)$ and the front point $F(x_f, y_f)$ are related by

$$x_f = x_r + l \cos \phi ; \quad y_f = y_r + l \sin \phi \quad (3)$$

where l denotes the distance between R and F , i.e., the rover length. Thus, the velocities of R and F are related by

$$\dot{x}_f = \dot{x}_r - l\dot{\phi} \sin \phi ; \quad \dot{y}_f = \dot{y}_r + l\dot{\phi} \cos \phi \quad (4)$$

From equations (2) and (4), we obtain the following *non-holonomic kinematic constraint*

$$\dot{x}_f \sin \phi - \dot{y}_f \cos \phi + \dot{\phi} l = 0 \quad (5)$$

or, in matrix form

$$[\sin \phi \quad -\cos \phi \quad l] \dot{p} = 0 \quad (6)$$

where $\dot{p} = [\dot{x}_f, \dot{y}_f, \dot{\phi}]^T$. Equation (6) represents a natural constraint that must be satisfied by the velocity vector \dot{p} , [7]. Note that equation (6) is a special form of the non-holonomic constraint

$$G(p)\dot{p} = 0 \quad (7)$$

where G is a $\nu \times n$ matrix and p is the $n \times 1$ vector of generalized coordinates of the system. A kinematic constraint of the form (7) is called non-holonomic if it is non-integrable; i.e., \dot{q} can not be eliminated and the constraint (7) can not be rewritten in terms of q alone in the form $H(q) = 0$. Otherwise, the constraint is called holonomic.

Now, the control variables of the rover are the linear speed v of the front wheels and the steering angle γ between the front wheels and the main axis of the rover. The control variables $[v, \gamma]$ are related to the velocity variables $[\dot{x}_f, \dot{y}_f, \dot{\phi}]$ by

$$\begin{aligned} \dot{x}_f &= v \cos(\phi + \gamma) \\ \dot{y}_f &= v \sin(\phi + \gamma) \\ \dot{\phi} &= \frac{v}{l} \sin \gamma \end{aligned} \quad (8)$$

where the third equation is derived from the first two and the constraint (6). Given $(\dot{x}_f, \dot{y}_f, \dot{\phi})$, the rover speed v and the steering angle γ are found from equation (8) as

$$v = \sqrt{\dot{x}_f^2 + \dot{y}_f^2}^{\frac{1}{2}} ; \quad \gamma = \sin^{-1} \left[\frac{\pm \dot{\phi} l}{(\dot{x}_f^2 + \dot{y}_f^2)^{\frac{1}{2}}} \right] \quad (9)$$

We conclude that at any configuration (x_f, y_f, ϕ) , the space of velocities $(\dot{x}_f, \dot{y}_f, \dot{\phi})$ achievable by the rover is restricted to a two-dimensional subspace in view of the constraint (6). This implies that the velocity vector \dot{p} is completely determined by the configuration vector p and, say, \dot{x}_f and \dot{y}_f . Notice that the achievable configuration space (x_f, y_f, ϕ) of the rover is three-dimensional, i.e., is completely unrestricted.

2.2 Holonomic Manipulator Subsystem

For simplicity of presentation, we consider a planar two-link manipulator arm mounted on the rover, as illustrated in Figure 1. However, the methodology presented in this paper is general and is equally applicable to any type of n -jointed rover-mounted manipulator.

Let θ_1 and θ_2 represent the joint angles and l_1 and l_2 denote the link lengths of the manipulator arm. Consider a moving vehicle frame $\{V\}$ with axes $(F\hat{x}, F\hat{y})$ attached to the rover at the front midpoint F . Let the position of the manipulator's end-effector E be the primary task variable of interest. Then, the Cartesian coordinates of E with respect to the vehicle frame $\{V\}$ can be expressed as

$$\begin{aligned} \hat{x}_e &= l_1 \cos \theta_1 + l_2 \cos(\theta_1 + \theta_2) \\ \hat{y}_e &= l_1 \sin \theta_1 + l_2 \sin(\theta_1 + \theta_2) \end{aligned} \quad (10)$$

The end-effector position coordinates $X_e = [x_e, y_e]^T$ relative to the world frame $\{W\}$ are given by

$$\begin{aligned} x_e &= x_f + l_1 \cos(\theta_1 + \phi) + l_2 \cos(\theta_1 + \theta_2 + \phi) \\ y_e &= y_f + l_1 \sin(\theta_1 + \phi) + l_2 \sin(\theta_1 + \theta_2 + \phi) \end{aligned} \quad (11)$$

From equation (11), the Cartesian velocity of the end-effector in $\{W\}$ is related to the rate-of-change of the configuration variables as

$$\begin{aligned} \dot{x}_e &= \dot{x}_f - l_1(\dot{\theta}_1 + \dot{\phi}) \sin(\theta_1 + \phi) \\ &\quad - l_2(\dot{\theta}_1 + \dot{\theta}_2 + \dot{\phi}) \sin(\theta_1 + \theta_2 + \phi) \\ \dot{y}_e &= \dot{y}_f + l_1(\dot{\theta}_1 + \dot{\phi}) \cos(\theta_1 + \phi) \\ &\quad + l_2(\dot{\theta}_1 + \dot{\theta}_2 + \dot{\phi}) \cos(\theta_1 + \theta_2 + \phi) \end{aligned} \quad (12)$$

or, in matrix form

$$\begin{bmatrix} 1 & 0 & J_{m13} & J_{m14} & -l_2 \sin \theta_{120} \\ 0 & 1 & J_{m23} & J_{m24} & l_2 \sin \theta_{120} \end{bmatrix} \begin{bmatrix} \dot{x}_e \\ \dot{y}_e \\ \dot{\phi} \\ \dot{\theta} \end{bmatrix} = \dot{X}_e \quad (13)$$

where $J_{m13} = J_{m14} = -l_1 \sin \theta_{10} - l_2 \sin \theta_{120}$, $J_{m23} = J_{m24} = l_1 \cos \theta_{10} + l_2 \cos \theta_{120}$, $\theta_{10} = \theta_1 + \phi$, $\theta_{120} = \theta_1 + \theta_2 + \phi$, and $\theta = [0, \theta_2]^T$ is the 2×1 manipulator's joint angle vector. Equation (13) can be written in the compact form

$$J_m(q)\dot{q} = \dot{X}_e \quad (14)$$

where $J_m(q)$ is the 2×5 manipulator's end-effector Jacobian matrix, and $q = [p^T, \theta^T]^T = [x_f, y_f, \phi, \theta_1, \theta_2]^T$ is the 5×1 configuration vector of the rover-mounted manipulator system. Equation (14) represents a *holonomic* kinematic constraint since it can be expressed as the position constraint $H(q) = 0$ in the form of equation (11).

We conclude that the kinematics of the rover-plus-manipulator system can be modeled as the non-holonomic rover constraint

$$J_r(q)\dot{q} = 0 \quad (15)$$

where $J_r(q) = [G'(p) : 0]$, together with the holonomic manipulator constraint

$$J_m(q)\dot{q} = \dot{X}_e \quad (16)$$

Equations (15) and (16) are combined to obtain the differential kinematic model of the integrated rover-plus-manipulator system as

$$\begin{bmatrix} J_r(q) \\ J_m(q) \end{bmatrix} \dot{q} = \begin{bmatrix} 0 \\ \dot{X}_e \end{bmatrix} \quad (17)$$

where the dimensions of \dot{q} and $[0, \dot{X}_e^T]^T$ are $n = 5$ and $m = 3$, respectively.

3 Motion Control of Rover-Manipulator System

In this section, the configuration control methodology developed earlier [14-15] for redundant manipulators is extended to motion control of the rover-plus-manipulator system.

Consider the integrated rover-plus-manipulator system. The integrated system in equation (17) is kinematically redundant with the degree-of-redundancy $r = 11 - m = 2$. In the configuration control approach, the

redundancy is utilized to accomplish *additional* user-specified tasks by direct control of a set of r user-defined kinematic functions

$$Z = g(q) \quad (18)$$

while controlling the end-effector motion, where Z and g are $r \times 1$ vectors. The additional task variables can be expressed in the velocity form

$$J_e(q)\dot{q} = \dot{Z} \quad (19)$$

where $J_e = \frac{\partial g}{\partial q}$ is the $r \times n$ Jacobian matrix associated with the kinematic functions Z . On combining the over-plus-manipulator constraints (17) and the user-specified additional task variables (19), we obtain

$$\begin{bmatrix} J_r(q) \\ J_m(q) \\ J_e(q) \end{bmatrix} \dot{q} = \begin{bmatrix} 0 \\ \dot{X}_e \\ \dot{Z} \end{bmatrix} \quad (20)$$

or, in matrix form

$$J(q)\dot{q} = \dot{X} \quad (21)$$

where $J(q)$ is the composite $n \times n$ Jacobian matrix, and $\dot{X} = [0, \dot{X}_e^T, \dot{Z}^T]^T$ is the $n \times 1$ task velocity vector.

Suppose that the desired end-effector velocity \dot{X}_{de} and the desired rate-of-variation of the kinematic functions \dot{Z}_d are specified by the user. Then we need to solve the augmented differential kinematic equation

$$J(q)\dot{q} = \dot{X}_d \quad (22)$$

for \dot{q} , where $\dot{X}_d = [0, \dot{X}_{de}^T, \dot{Z}_d^T]^T$. To avoid large velocities \dot{q} , the user can impose the velocity weighting factor $W_v = \text{diag}\{W_a, W_b\}$ on $\{\dot{p}, \dot{\theta}\}$, and attempt to minimize the weighted sum-of-squares of velocities $\|\dot{p}\|_{W_a}^2 + \|\dot{\theta}\|_{W_b}^2$. In addition, the user can assign priorities to the end-effector motion, the additional task requirements, and the non-holonomic rover constraint by selecting the appropriate task weighting factor $W_t = \text{diag}\{W_r, W_e, W_c\}$, and seek to minimize the weighted sum of task velocity errors $\|\dot{E}_r\|_{W_r}^2 + \|\dot{E}_e\|_{W_e}^2 + \|\dot{E}_c\|_{W_c}^2$, where $\dot{E}_r = J_r\dot{q}$, $\dot{E}_e = \dot{X}_{de} - \dot{X}_e$ and $\dot{E}_c = \dot{Z}_d - \dot{Z}$ are the non-holonomic rover, end-effector, and additional task velocity errors, respectively. Hence, we seek to find the optimal solution of equation (22) that minimizes the scalar cost function

$$I = \dot{p}^T W_a \dot{p} + \dot{\theta}^T W_b \dot{\theta} + \dot{E}_r^T W_r \dot{E}_r + \dot{E}_e^T W_e \dot{E}_e + \dot{E}_c^T W_c \dot{E}_c \quad (23)$$

The optimal damped-least-squares solution of (22) that minimizes (23) is given by [15]

$$\dot{q} = [J^T W_t J + I W_v]^{-1} J^T W_t \dot{X}_d \quad (24)$$

This solution is singularity-robust for $W_v \neq 0$, since the matrix inverted is always positive-definite and hence non-singular. Note that in the special case where $W_v = 0$, equation (24) gives $\dot{q} = J^{-1} \dot{X}_d$, assuming $\det[J] \neq 0$, which is the classical inverse Jacobian solution. To correct for task-space trajectory drift which can occur in differential kinematic schemes, we introduce the *actual* configuration vector X in equation (24) as [15]

$$\dot{q} = [J^T W_t J + W_v]^{-1} J^T W_t [\dot{X}_d + K(X_d - X)] \quad (25)$$

where K is an $n \times n$ constant diagonal matrix with zero or positive diagonal elements. Notice that for the non-holonomic rover constraint, the appropriate elements of X and X_d are set to zero since the constraint is non-integrable. The numerical value of K determines the rate of convergence of X to X_d .

Let us now re-visit the two-jointed manipulator arm mounted on the rover as illustrated in Figure 1. There are five degrees-of-freedom and only two end-effector coordinates to be controlled and one non-holonomic rover constraint to be satisfied. Therefore, two *additional* configuration-dependent kinematic functions $z_1(q)$ and $z_2(q)$ can be specified and controlled independently of the end-effector motion and the non-holonomic rover constraint. For the sake of illustration, we choose the rover orientation ϕ relative to the world frame and the manipulator elbow angle ψ between the upper-arm and forearm as the additional task variables. Hence

$$z_1(q) = \phi; \quad z_2(q) = \psi = 180^\circ - \theta_2 \quad (26)$$

or, in velocity form

$$\begin{bmatrix} 0 & 0 & 1 & 0 & 0 \\ 0 & 0 & 0 & 0 & -1 \end{bmatrix} \dot{q} = \begin{bmatrix} \dot{\phi}_d \\ \dot{\psi}_d \end{bmatrix} \quad (27)$$

where $\dot{q} = [\dot{x}_t, \dot{y}_t, \dot{\phi}, \dot{\theta}_1, \dot{\theta}_2]^T$, and $\dot{\phi}_d$ and $\dot{\psi}_d$ are the desired rate-of-variation of ϕ and ψ , respectively. On combining the rover-plus-manipulator model (1') with the additional task specifications (27), we obtain

$$\begin{bmatrix} \sin \phi & -\cos \phi & 1 & 0 & 0 \\ 1 & 0 & J_{23} & J_{24} & J_{25} \\ 0 & 1 & J_{33} & J_{34} & J_{35} \\ 0 & 0 & 1 & 0 & 0 \\ 0 & 0 & 0 & 0 & -1 \end{bmatrix} \begin{bmatrix} \dot{x}_f \\ \dot{y}_f \\ \dot{\phi} \\ \dot{\theta}_1 \\ \dot{\theta}_2 \end{bmatrix} = \begin{bmatrix} 0 \\ \dot{x}_{de} \\ \dot{y}_{de} \\ \dot{\phi}_d \\ \dot{\psi}_d \end{bmatrix} \quad (28)$$

where $J_{23} = J_{24} = -l_1 \sin \theta_{10} - l_2 \sin \theta_{120}$; $J_{33} = J_{34} = l_1 \cos \theta_{10} + l_2 \cos \theta_{120}$; $J_{25} = -l_2 \sin \theta_{120}$; $J_{35} = l_2 \cos \theta_{120}$; $\theta_{10} = \theta_1 + \phi$; $\theta_{120} = \theta_1 + \theta_2 + \phi$. Note that (28) embodies the non-holonomic rover constraint (5). Equation (28) represents a set of five equations in

the five unknown elements of \dot{q} that can be solved using the damped-least-squares configuration control approach described earlier in this section. By direction calculation, the determinant of the 5×5 augmented Jacobian matrix appearing on the left-hand side of (28) is found to be

$$\det[J] = l_1 \cos \theta_1 + l_2 \cos(\theta_1 + \theta_2) = \hat{x}_e \quad (29)$$

Therefore, J is non-singular and (28) can be solved exactly provided that $\hat{x}_e \neq 0$; i.e., the end-effector F does not lie on the $F\hat{y}$ axis of the vehicle frame $\{V\}$.

Now, suppose that the rover length is $l = 20$ cm and the link lengths are $l_1 = l_2 = 10$ cm. Let the initial configuration of the rover-plus-manipulator system be given by

$$q^i = \{x_f = 30 \text{ cm}, y_f = 15 \text{ cm}, \phi = 0^\circ, \theta_1 = -75^\circ, \theta_2 = 150^\circ\}$$

This yields the initial task vector

$$X^i = \{x_e = 35.18 \text{ cm}, y_e = 15 \text{ cm}, \phi = 0^\circ, \psi = 30^\circ\}$$

Suppose that the desired final task vector at time $\tau = 1$ second is specified as

$$X^f = \{x_e = 65.18 \text{ cm}, y_e = 45 \text{ cm}, \phi = 30^\circ, \psi = 90^\circ\}$$

This corresponds to a rapid end-effector motion of $\{(\Delta x_e)^2 + (\Delta y_e)^2\}^{1/2} = 42.4$ cm in one second. Notice that the target end-effector position is *not* attainable without rover motion. Task-space motion trajectories are specified as straight-lines; for instance

$$x_d(t) = \begin{cases} x^i + \frac{x^f - x^i}{\tau} \cdot t & \text{for } t \leq \tau \\ x^f & \text{for } t > \tau \end{cases} \quad (30)$$

where (x^i, x^f) are the initial and final values and τ is the duration of motion. Similar trajectories are specified for $y_d(t)$, $\phi_d(t)$, and $\psi_d(t)$. These trajectories produce a straight-line end-effector motion in Cartesian space from (x_e^i, y_e^i) to (x_e^f, y_e^f) . Notice that the target elbow angle $\psi = 90^\circ$ gives maximum end-effector manipulability at the final configuration.

A computer simulation study is performed to calculate the required configuration variables $q(t) = \{x_f(t), y_f(t), \phi(t), \theta_1(t), \theta_2(t)\}$ to accomplish the tasks of end-effector motion, and ϕ and ψ control, while satisfying the non-holonomic rover constraint. In the simulation, we set $\tau = 1$. At $t = 0.01$, $W_t = \text{diag}\{1, 1, 1, 1, 1\}$, $W_v = \text{diag}\{0, 0, 0, 0, 0\}$, and $K = \text{diag}\{0, 0.1, 0.1, 0, 0\}$. The simulation results are shown in Figures 2a-2b. The path traversed by the end-effector F is shown in Figure 2a. It is seen that the end-effector moves on a straight line from (x_e^i, y_e^i) to (x_e^f, y_e^f) , as

specified. Figure 2b verifies that the rover orientation ϕ and the elbow angle ψ change from their initial values to the specified final values on straight-lines in one second, as desired. The non-holonomic rover constraint function $f = \dot{x}_f \sin \phi - \dot{y}_f \cos \phi + \dot{\phi}l$ is computed and found to be equal to zero throughout the motion; i.e., the rover constraint, is satisfied. Note that the required rover speed v and steering angle γ can be computed from equation (9).

4 Conclusions

A simple scheme is presented for on-line control of rover-mounted manipulators. The configuration control approach is extended to incorporate the non-holonomic rover constraint with the desired end-effector motion and the user-specified redundancy resolution goals. The key advantages of the present approach over the previous schemes are its flexibility, simplicity, and computational efficiency. The ability to change the task specifications and the task weighting factors on-line based on the user requirements provides a flexible framework for mobile robot control. Furthermore, in contrast to previous approaches which are suitable for off-line motion planning, the simplicity of the present approach leads to computational efficiency which is essential for on-line control in real-time implementations.

References

- [1] W. F. Carriker, P. K. Khosla, and B. H. Krogh: "Path planning for mobile manipulators for multiple task execution," *IEEE Trans. on Robotics and Automation*, Vol. 7, No.3, pp. 403-408, June 1991.
- [2] W. F. Carriker, P. K. Khosla, and H. H. Krogh: "The use of simulated annealing to solve the mobile manipulator path planning problem," *Proc. IEEE Intern. Conf. on Robotics and Automation*, pp. 204-209, May 1990.
- [3] F. G. Pin and J. C. Culioli: "Optimal positioning of redundant manipulator - platform systems for maximum task efficiency," *Proc. Intern. Symposium on Robotics and Manufacturing* pp. 489-495, July 1990.
- [4] F. G. Pin and J. C. Culioli: "Multi-criteria position and configuration optimization for redundant platform/manipulator systems," *Proc. IEEE Workshop on Intelligent Robots and Systems*, pp. 103-107, July 1990.
- [5] N. A. M. Hootsmans and S. Dubowsky: "Large motion control of mobile manipulators including vehicle suspension characteristics," *Proc. IEEE Intern. Conf. on Robotics and Automation*, pp. 233&2341, April 1991.
- [6] H. Seraji: "An on-line approach to coordinated mobility and manipulation," *Proc. IEEE Intern. Conf. on Robotics and Automation*, Vol. 1, pp. 28-35, Atlanta, May 1993.
- [7] J. Barraquand and J. C. Latombe: "On nonholonomic mobile robots and optimal maneuvering," *Proc. 4th IEEE Intern. Symposium on Intelligent Control*, pp. 340-347, Albany, September 1989.
- [8] Y. Yamamoto and X. Yun: "Coordinating locomotion and manipulation of a mobile manipulator," *Proc. 31st IEEE Conf. on Decision and Control*, pp. 2643-2648, Tucson, December 1992.
- [9] Y. Yamamoto and X. Yun: "Control of mobile manipulators following a moving surface," *Proc. IEEE Intern. Conf. on Robotics and Automation*, Vol. 3, pp. 1-6, Atlanta, May 1993.
- [10] C. C. Wang, N. Sarkar, and V. Kumar: "Rate kinematics of mobile manipulators," *Proc. 22nd Biennial ASME Mechanisms Conf.*, pp. 225-232, Scottsdale, September 1992.
- [11] C. C. Wang and V. Kumar: "Velocity control of mobile manipulators," *Proc. IEEE intern. Conf. on Robotics and Automation*, Vol. 2, pp. 713-718, Atlanta, May 1993.
- [12] K. Liu and F. J. Lewis: "Control of mobile robot with onboard manipulator," *Proc. Intern. Symposium on Robotics and Manufacturing*, Vol. 4, pp. 539-146, Santa Fe, November 1992.
- [13] S. Jagannathan, F. J. Lewis, and K. Liu: "Modeling, control and obstacle avoidance of a mobile robot with an onboard manipulator," *Proc. IEEE Intern. Symp. on Intelligent Control*, Chicago, August 1993.
- [14] H. Seraji: "Configuration control of redundant manipulators: Theory and implementation," *IEEE Trans. on Robotics and Automation*, Vol. 5, No. 4, pp. 472-490, 1989.
- [15] H. Seraji and R. Colbaugh: "Improved configuration control for redundant robots," *Journal of Robotic Systems*, Vol. 7, No. 6, pp. 897-928, 1990.

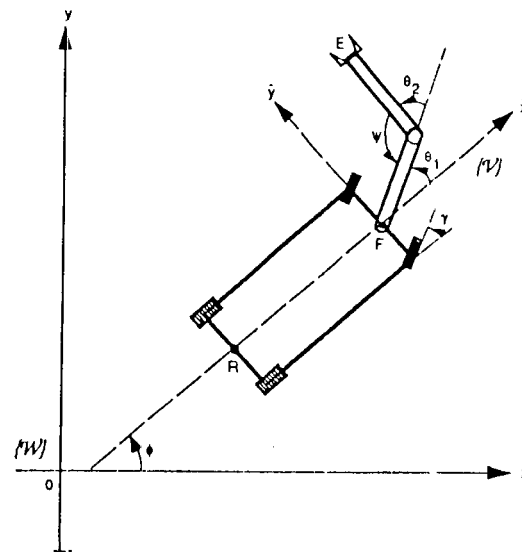


Figure 1. Rover-mounted manipulator

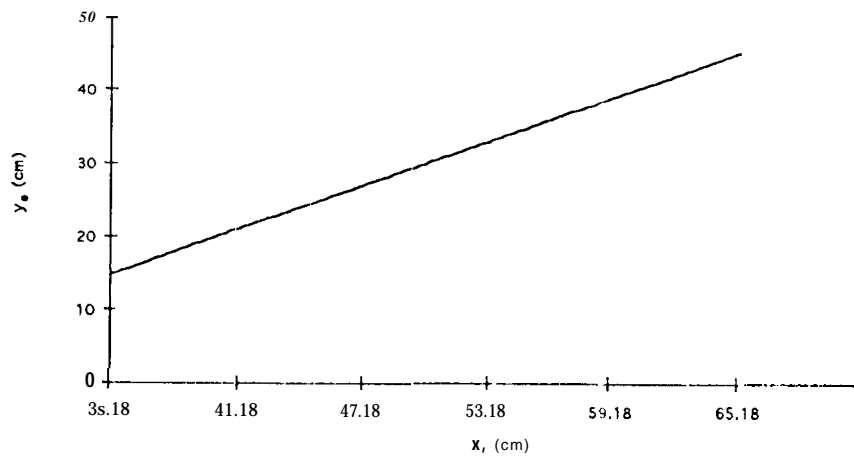


Figure 2a. Motion trajectory of the end-effector E

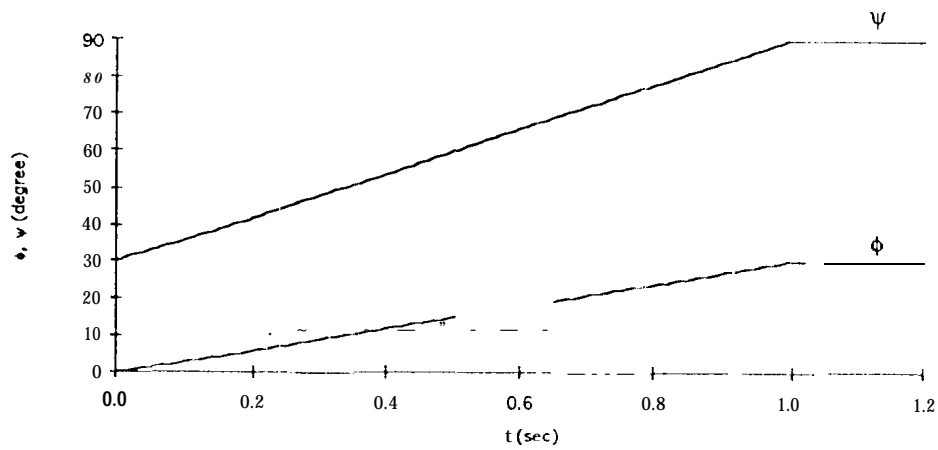


Figure 2b. Variations of the rover orientation ϕ and elbow angle ψ